UHASSELT
KNOWLEDGE IN ACTION

Faculteit Wetenschappen

master in materiomics

Masterthesis

Pulsed Protocol Design and Optimization for Eddy Current based Material Analysis using Diamond Quantum Sensors

Tom Cornille
Scriptie ingediend tot het behalen van de graad van master in materiomics

PROMOTOR :
dr. Jaroslav HRUBY
Prof. dr. Anna ERMAKOVA

UHASSELT
KNOWLEDGE IN ACTION

www.uhasselt.be
Universiteit Hasselt
Campus Hasselt:
Martelarenlaan 42 | 3500 Hasselt
Campus Diepenbeek:
Agoralaan Gebouw D | 3590 Diepenbeek

2023
2024

Faculteit Wetenschappen

master in materiomics

Masterthesis

Pulsed Protocol Design and Optimization for Eddy Current based Material Analysis using Diamond Quantum Sensors

Tom Cornille

Scriptie ingediend tot het behalen van de graad van master in materiomics

PROMOTOR :
dr. Jaroslav HRUBY
Prof. dr. Anna ERMAKOVA

Pulsed Protocol Design and Optimization for Eddy Current based Material Analysis using Diamond Quantum Sensors

Tom Cornille[1,2,*], *Anna Ermakova*[1,2,3] *and Jaroslav Hruby*[1,2]

[1] Hasselt University, Agoralaan gebouw D, 3590 Diepenbeek, Belgium.

[2] IMO-IMOMEC Institute for Material Research (IMO), Wetenschapspark 1, 3590 Diepenbeek, Belgium

[3] Belgian Institute for Space Aeronomy (BIRA-IASB), Ringlaan 3, 1180 Ukkel, Belgium.

E-mail: tom.cornille@student.uhasselt.be

jaroslav.hruby@uhasselt.be

anna.ermakova@uhasselt.be

Keywords: Time-resolved Eddy current, Quantum sensor, Pulsed protocols, Nitrogen-Vacancy centers.

Abstract

Colonizing the lunar surface has its challenges due to the harsh environment (radiation, temperature, dust), limited energy sources, and high costs of material to orbit. That is why in situ mining is considered for these expeditions. This requires the preselection of raw materials for refining. This can be enabled by Time-resolved Eddy current detection methodology utilizing a portable quantum diamond sensor, operated in the pulse regime

Nitrogen-Vacancy centers have emerged as a promising sensor due to their opto-magnetic properties and temperature stability. Combined with a theoretical sub-pico tesla sensitivity and fast response to changes in the magnetic field, it can perform material characterization using non-destructive Eddy currents. From the decay pattern of these currents, information about the conductivity and (magnetic) permeability can be determined.

First, a Rabi measurement study is performed to optimize the system boundary conditions and pulse scheme. From these results, the π-pulse times are extracted at different microwave powers. At the highest power of 20 dBm, the optimal pulse duration is 700 ns. This is then implemented in the time-resolved Eddy current measurement, to investigate the decay at an increased sensitivity. The shift in intensity between measurements with and without a conductive sample is observed, proving the concept.

Abstract (Nederlandstalig)

Het maanoppervlak koloniseren heeft zo zijn uitdagingen door de harde omgeving (straling, temperatuur, stof), beperkte energiebronnen en hoge kosten om materiaal in een baan om de aarde te brengen. Daarom wordt voor deze expedities in situ mijnbouw overwogen. Dit vereist de voorselectie van grondstoffen voor raffinage. Dit kan mogelijk worden gemaakt door tijdgeresolveerde wervelstroomdetectie met behulp van een draagbare kwantumdiamantsensor die in het pulsregime werkt.

Stikstof-vacature centra zijn naar voren gekomen als een veelbelovende sensor vanwege hun opto-magnetische eigenschappen en temperatuurstabiliteit. Gecombineerd met een theoretische sub-pico tesla gevoeligheid en snelle respons op veranderingen in het magnetische veld, kan het materiaalkarakterisering uitvoeren met behulp van niet-destructieve Eddy-stromen. Uit het vervalpatroon van deze stromen kan informatie over de geleidbaarheid en (magnetische) permeabiliteit worden bepaald.

Eerst wordt een Rabi-meetstudie uitgevoerd om de randvoorwaarden van het systeem en het pulsschema te optimaliseren. Uit deze resultaten worden de π-pulstijden gehaald bij verschillende microgolfvermogens. Bij het hoogste vermogen van 20 dBm is de optimale pulsduur 700 ns. Dit wordt vervolgens geïmplementeerd in de tijdgeresolveerde Eddystroommeting om het verval bij een verhoogde gevoeligheid te onderzoeken. De verschuiving in intensiteit tussen metingen met en zonder een geleidend monster wordt waargenomen, wat het concept aantoond.

1. Introduction

The harsh environment, limited energy, and high costs of rocket launching are significant factors that should be taken into account during any space experiment. [1] Focussing on colonization efforts, building habitats on the surface of celestial bodies is not an easy task. It is not possible to transport all the necessary materials via rockets, so a creative solution needs to be found. To solve this problem, this work/paper suggests using a quantum sensor based on Nitrogen-Vacancy centers in diamond for in-situ mining of minerals by detecting Eddy currents.

Eddy currents (EC) are a non-destructive measuring technique that operates by measuring the magnetic fields produced by an induced current, called secondary fields. The induced current is generated according to Lenz's law by applying an alternating external magnetic field, called the primary field, to a conductive material using a coil. There are two ways to monitor this effect. Either measure the resulting magnetic fields directly or investigate how the current running through the coil is altered when the secondary field reacts with it. Since the ultimate goal is to prove that quantum sensor based on diamond can detect these ECs, the former monitoring technique is used. [1–3]

There are many variables that determine the material's response to this primary alternating field, they can be categorized into three groups: inspection system, material properties, and testing conditions. The inspection system and testing condition variables can be summarized as the frequency of the alternating external field, the distance between the coil and the sample (called lift-off), the strength of the external field, and the operating mode (continuous or pulsed excitation). By controlling these variables and analyzing the corresponding EC through the secondary magnetic field, information about material properties can be found: defects, thickness, composition, conductivity, and permeability of conductive samples. [1–4]

Ultimately, the goal of this work is to use Time-Resolved Eddy Current (TREC) measurements to investigate conductivity and permeability measurements, determine the composition of conductive samples, and distinguish them by composition. TREC is a pulsed technique that investigates the EC decay over time, enabling materials characterization. In this manner, the method can be used to preselect materials in situ for refining and reducing costs. Additionally, this method is non-invasive and not hazardous while operated, and it is capable of providing instant results. This makes this technique a promising candidate for space applications. However, the influence of harsh environmental issues is still uninvestigated. [5–7]

That is why diamond is proposed as the magnetic sensor. Its hardness, temperature/radiation resistance, and photostability are ideal for space's unforgiving environment. [8,9]

Nitrogen-Vacancy (NV) centers are defects in the diamond lattice with unique opto-magnetic properties. This means that it is possible to manipulate electron spin states by an external microwave field and optically measure these spin states because their fluorescence is spin-dependent. This measuring technique is called Optically Detected Magnetic Resonance (ODMR). The optical excitation is made by a green laser. The readout of the system is done by detecting red photoluminescence and analyzing light intensities. These spin states are sensitive to the Zeeman effect, which can be used to observe an external magnetic field. This makes NV-centers a quantum sensor. [5,6,10–16] As for the EC technique, these measurements can be taken continuously or via pulsed methods. The first technique is considered easy to realize but has drawbacks in heat generation and sensitivity. Despite not being used to perform the final measurement, it is useful when building the entire measuring system. The second requires the pulsing of the laser and microwave field for a well-defined amount of time at a specific microwave frequency. When performed correctly, it manipulates the spin states in a controlled manner, maximizing the contrast of red light emission between on- and off-resonant microwave fields. Additionally, the ODMR linewidth is decreased, resulting in better magnetic field sensitivity. [12] In this work, Rabi measurements are performed to find the optimal pulse durations of the microwave and laser for subsequent measurements, such as pulsed ODMR and TREC measurements.

This study proposes a device that will detect ECs using a quantum sensor. By measuring conductivity and magnetic permeability, materials can be distinguished and preselected for refining. This will significantly reduce purifying costs and increase energy efficiency. Despite being investigated for space applications, this science can also be practical here on Earth. Since it revolves around scanning conductive materials, it can be used to filter precious metals from (electronic) landfills, reducing refining costs, similar to space applications. Some metals are diminishing in abundance, so recycling these will, at one point, be necessary.

2. Experimental setup

2.1. Testbench

Performing this study requires the construction of a new working station or testbench; see **Figure 1**. The layout can be divided into two segments. The first discusses the readout components of the magnetometer while the second represents the equipment needed for EC generation.

The **magnetometer system** includes a green diode laser (520 nm, OSCAR-Lab) with a collimation lens to illuminate the diamond surface. Next, the laser light is guided through a hot mirror (FM02, Thorlabs) that is transparent for green light and reflects red light. Then the laser is focussed onto the diamond where red photoluminescent light is emitted. The emitted light reflects from the hot mirror and passes through a 650 nm long-pass filter (FELH0650, Thorlabs) before being detected by an avalanche photodiode (APD120A/M, Thorlabs). The laser and diamond subsystems will be individually discussed in section 2.2 and 2.3 as they require additional characterization. To measure magnetic fields, two more components are required, a microwave field and a magnetic field. A microwave generator (SynthHD mini, Windfreak Technologies) is used to apply the field to the system using an antenna (ø 25 µm Aluminium wirebonding wire) that is located on the diamond surface. This device is used in a range from 2700 to 3050 MHz and at an output power between -16 to 20 dBm. Lastly, a magnetic field is applied to the system to fully split all individual peaks. This is done either via a permanent magnet or an electromagnet. In this study, a permanent magnet is used. Complete splitting of the ODMR peaks is necessary to measure absolute magnetic fields.

To make the handling of these components more streamlined, a LabVIEW program was developed during this work. The code is capable of performing ODMR, Rabi, pulsed ODMR, and EC measurements. On top of that, it is capable of adjusting the laser and microwave settings. Since these experiments require that the laser and microwaves are pulsed, a pulse generator (BNC588, Berkeley Nucleonics) is added. It can be directly connected to the homemade laser board, but to control the microwave generator, a microwave switch (ZASWA-2-50DRA+, Minicircuits) is implemented. The pulse generator can also be controlled using the LabVIEW program.

The **Eddy current system** requires a conductive material, a coil, and a way to pulse the current. Gold was directly deposited on top of the diamond surface to make the conductive sample, see **Figure 2**. It was done by photolithography, where initially, a layer of 20 nm titanium was deposited on the diamond surface, and then a second gold layer with 100 nm thickness was placed on top of it, see Figure 2. The diamond sample was then cleaned in acetone and isopropanol. The coil is made using a copper wire with a 50 µm diameter with a total of 10 windings. It has a diameter of 0.965 cm and the length is 1 mm. It is placed between the diamond and the focusing lens.

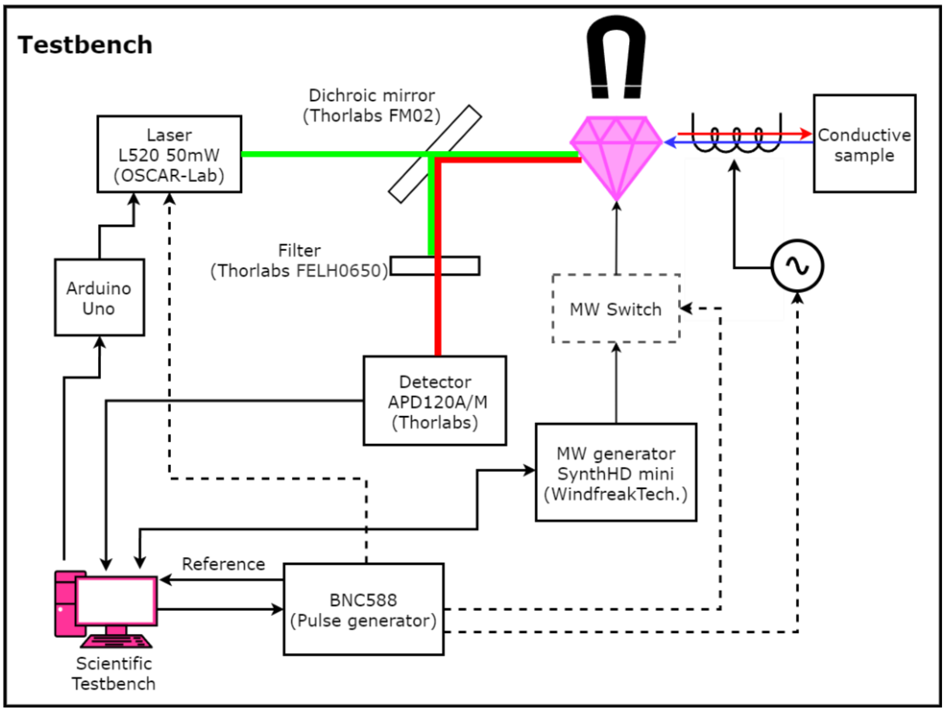

Figure 1: Representation of the testbench used to perform all measurements. The Eddy current coil, power source, and switch were installed after the rabi measurements were verified.

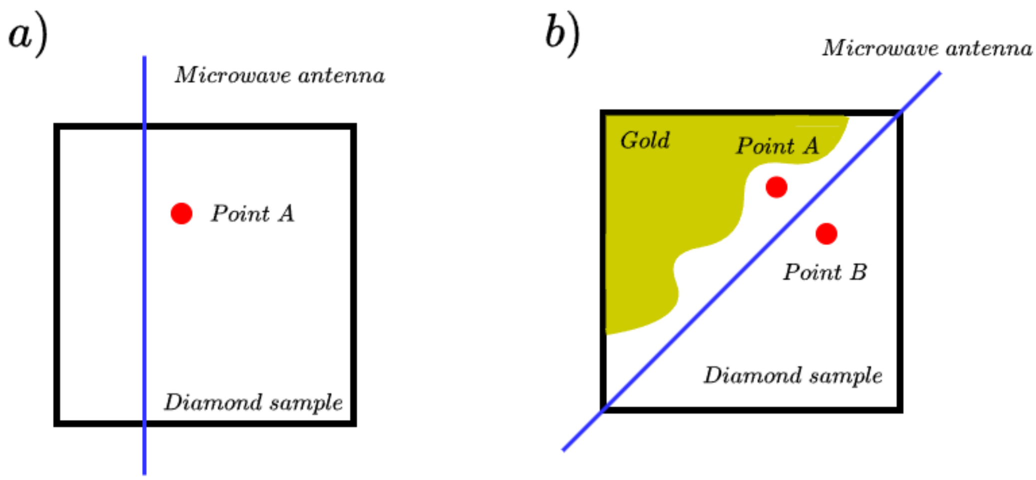

Figure 2: A top view representation of the diamond surface that is a) uncoated, and b) partially coated with a gold conductive layer. A microwave antenna is placed over the non-coated region and measurements are performed on equidistant locations from the antenna.

2.2 Laser properties

Since the laser diode and its controls are self-made, a study has been conducted to determine their characteristics. The laser is controlled by a LabVIEW program that gives commands to a microcontroller (Arduino UNO). However, the inputs of the microcontroller do not have a linear relation to the generated laser power. The range of the Arduino is from 0 to 1023. However, at an Arduino output, around 400, the laser power becomes negligible, see Figure 3a. Due to this, the investigated Arduino range is limited between 0 and 400 with a step size of 20. Figure 3 shows how the laser power, current consumption, and sensor temperature relate to the output provided by the Arduino, where 0 corresponds to full power of 50 mW, a current of 0.2 A, and a maximum temperature of 36 °C. The majority of the pulse measurements were performed at 45 mW to avoid overheating. While the diamond characterization is executed using 30 mW of laser power.

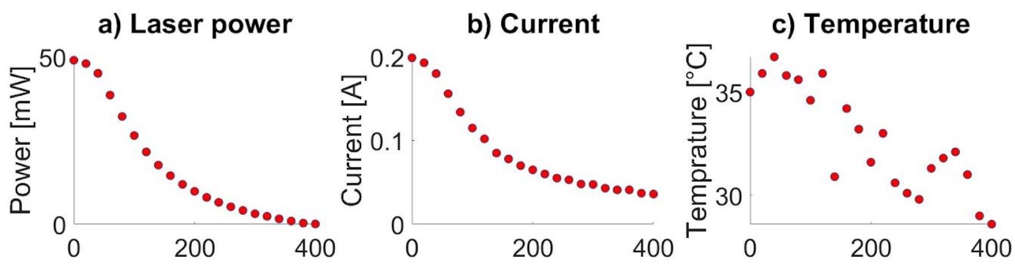

Figure 3: The laser properties at different working points produced by an Arduino. a) Laser power produced between Arduino output 0 and 400, b) Current, and c) temperature dependency.

2.3. Diamond properties

Similar to the laser, the diamond that will be used for sensing should also be investigated. Here, three samples are investigated: ‘405’, ‘472’, and ‘480’. Sample ‘405’ is purchased from Thorlabs, has an NV center concentration of 4.5 ppb, and is created via Chemical Vapor Deposition. Sample ‘472’, also from Thorlabs, has a concentration of 300 ppb and is irradiated. Sample ‘480’ from MSE pro, has a concentration >100 ppb.

But what defines a good sensor? There are three main characteristic parameters, namely contrast between the maximum and minimum light intensity, Full Width Half Max (FWHM) of the ODMR spectrum, and base intensity which is the emission when off-resonance microwaves are applied.

Additionally, to most accurately compare different samples, they should be investigated under multiple conditions, for example, magnetically splitted and unsplitted, and at different microwave powers.

Figure 4 shows two sets of data. a), b), and c) represent unsplitted data, meaning without a magnetic field present. Here, the data is acquired with a high laser power of ~ 30 mW and high microwave amplification (16 dBm). The results of the different samples are then compared to each other.

Figures 4 d), e), and f) show splitted data, where a permanent magnet was used, measured under different conditions. The full lines represent data acquired a higher laser power of ~ 30 mW while the dashed lines are made at a lower laser power of ~ 10 mW. Additionally, the microwave power is adjusted between 16, 0, and -16 dBm.

When looking at the unsplitted data, it is visible that Sample ‘405’ is most optimal. It has the highest contrast, making the difference between on- and off-resonance microwave fields most visible. Also, the base intensity is highest, resulting in more light being emitted, which makes for easier detection. Lastly, the FWHM is lowest, meaning that measurements of higher accuracy can be performed. However, to make the conclusion that sample 405 is the most favorable, it should behave homogeneously in splitted regime and under different conditions. Luckily, this is generally the case. For the base intensity measurement, ‘405’ performs best under any condition. The contrast at high laser power is also highest for ‘405’. However, at lower laser and high microwave powers, sample ‘472’ performs better, but since the pulsed measurements are performed at higher laser powers, ‘405 is still preferred. Lastly, the FWHM of the ‘472’ sample is best at higher microwave powers. Since sample ‘405’ generally performs best, the rest of this study is conducted using this diamond.

Since for the time-resolved EC measurements, a conductive sample is needed, a diamond with the same characteristics is modified with a conductive layer on the surface, as described in the previous section.

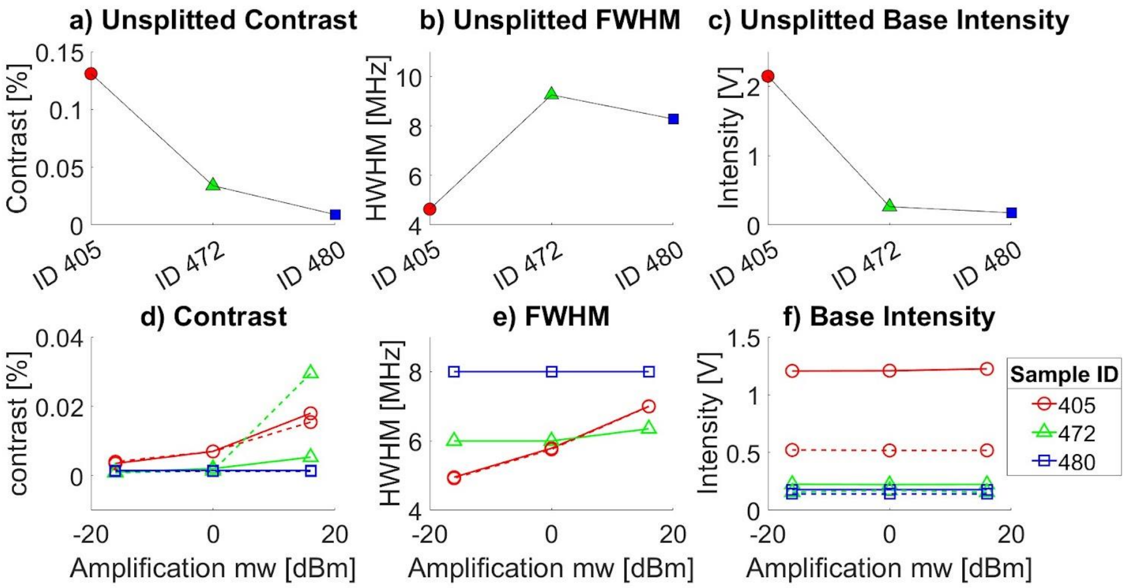

Figure 4: a) and d) show the contrast between the highest and lowest emitted intensity of three different samples in respectively magnetically unsplitted and splitted conditions. b) and e) are the FWHM of the (un)splitted data. Note that for sample 480 under splitted conditions, the FWHM was the highest and showed no real sign of improvement. Lastly, c) and f) are the base intensities under (un) splitted conditions.

2.4 Pulse schemes

As mentioned above, both the laser, microwave, and the coil current will be pulsed. This requires different schemes for each of the performed measurements, Rabi, Pulsed ODMR, and TREC. For all three experiments, both the laser and microwave are pulsed while the coil is only operated during TREC measurements. It should be noted that all pulse procedures are performed at full laser power, ~ 45-50 mW, and that two diamond samples are used. For the Rabi measurements, sample '405' is used while uncoated. The EC measurements are performed on a gold-coated diamond with the same characteristics. Lastly, the pulsed ODMR experiments are performed on both samples.

2.4.1. Rabi

In Rabi experiments, a microwave (MW) pulse at different durations (Tau) is applied to an initialized system, see **Figure 6a**. Note that the laser functions both as a readout mechanism and as initialization for the next iteration. The changing variable in this experiment is the duration of the microwave pulse. Depending on the duration, a large or small portion of the spin population is transitioned to another state, which affects the light intensity.

The frequency at which this pulse is applied is determined by analyzing continuous wave (CW) ODMR and extracting the frequency of the peak with the highest contrast.

Before performing Rabi experiments, the most optimal pulse scheme should be found. To do this, the time between microwave and laser pulse (X), and the time between iterations (Y) is investigated; see Figure 6a. Here, the chosen X-times to investigate were 0 ns, 150 ns, 300 ns, and 600 ns at a microwave power of 20 dBm, see **Figure 5**. There are two effects that can influence the data. First, the pulses are not a perfect square function. Near the beginning and end, they experience a rising/lowering edge. This can cause pulse overlap between the microwave and laser, which is not wanted as it distorts measurements. Second, if the gap is too big, T1 relaxation processes can already take place. T1 is the spontaneous relaxation of spin states.

It is determined that a MW-laser delay (X) of 300 ns performs best with a 500 ns delay at the end (Y). With the now-determined pulse scheme, Rabi measurements can be performed and other variables can be inspected, such as laser power, MW frequency and power used during the experiment, and temperature drifts. These will be discussed in the results section.

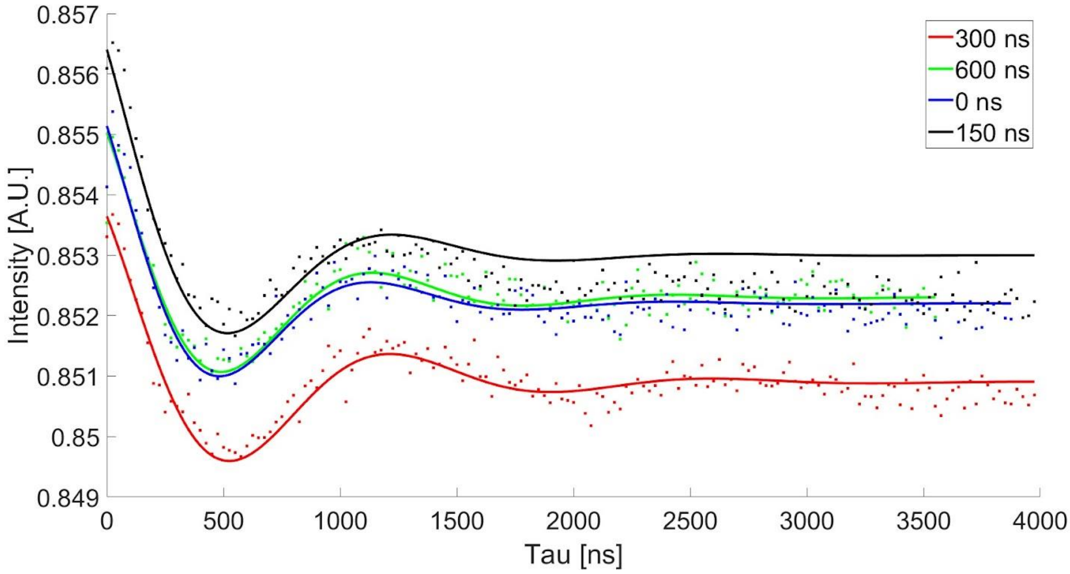

Figure 5: *Rabi measurements were performed with different delays between the microwave and laser pulse , see Figure 6a variable X. A delay of 300 ns (red), 600 ns (green), 0 ns (blue), and 150 ns (black) are tested.*

2.4.2. Pulsed ODMR

Pulsed ODMR is similar to a CW measurement, with the only difference being an initialization step. In this step, a microwave π-pulse is applied to the diamond sensor to manipulate as many spin states in order to produce the optical signal with the highest contrast. The experimental scheme is shown in Figure 6b. The frequency and length of the applied π-pulse are determined from the Rabi measurements. However, the real microwave frequency responsible for this transition will change during the measurement.

As discussed in the Rabi section, the manipulation of spin-states is very dependent on the correct frequency. So when an off-resonant frequency is used, the change in spin population will drastically reduce compared to on resonance. This results in dips in the ODMR spectra with lower FWHM while increasing the contrast.

To verify that the experiment succeeded, the contrast and FWHM will be compared to CW ODMR spectrums performed at different microwave powers. These powers depend on pulsed ODMR variables, such as the MW power used and the duty cycle. This is the ratio of time that the microwave is on compared to the total time of one cycle. Since the microwave is not turned on continuously, the effective power output is reduced according to this duty cycle. This results in an ODMR spectrum with a power-broadening effect related to a lower output power without significantly affecting the contrast. [17]

The aim of this experiment is to show that the Rabi measurements were correct and that the extracted π-pulse lengths are accurate.

2.4.3. Eddy Current

The pulsed EC scheme is very similar to that of the pulsed ODMR, see Figure 6c. The first difference is the timescale of the entire cycle. Since ECs are not formed instantaneously, the times are increased to the order of ms. [7] The second and most important difference is the pulsing of the current that flows through the coil. The pulse width is kept constant at 2 ms. The changing variable in this measurement is the delay at which the pulse starts. By moving it to the left, the pulse will be further from the next iteration, where the EC-induced magnetic field will be measured.

With this scheme, the Eddy current measurements can be performed. First, a measurement is taken to show that the effect of the coil is visible. This diamond sample is not preprocessed with aluminum and gold. Next, the processed sample is installed, and Rabi together with EC measurements are performed at two different locations on the diamond surface. Since the change in magnetic field is under investigation, the location of the laser spot matters. One measurement will be performed more closely to the gold layer, while a second is taken further away, see Figure 2. Note that it is important that the two laser spot locations are equidistant from the microwave antenna to make sure that the Rabi oscillations are the same.

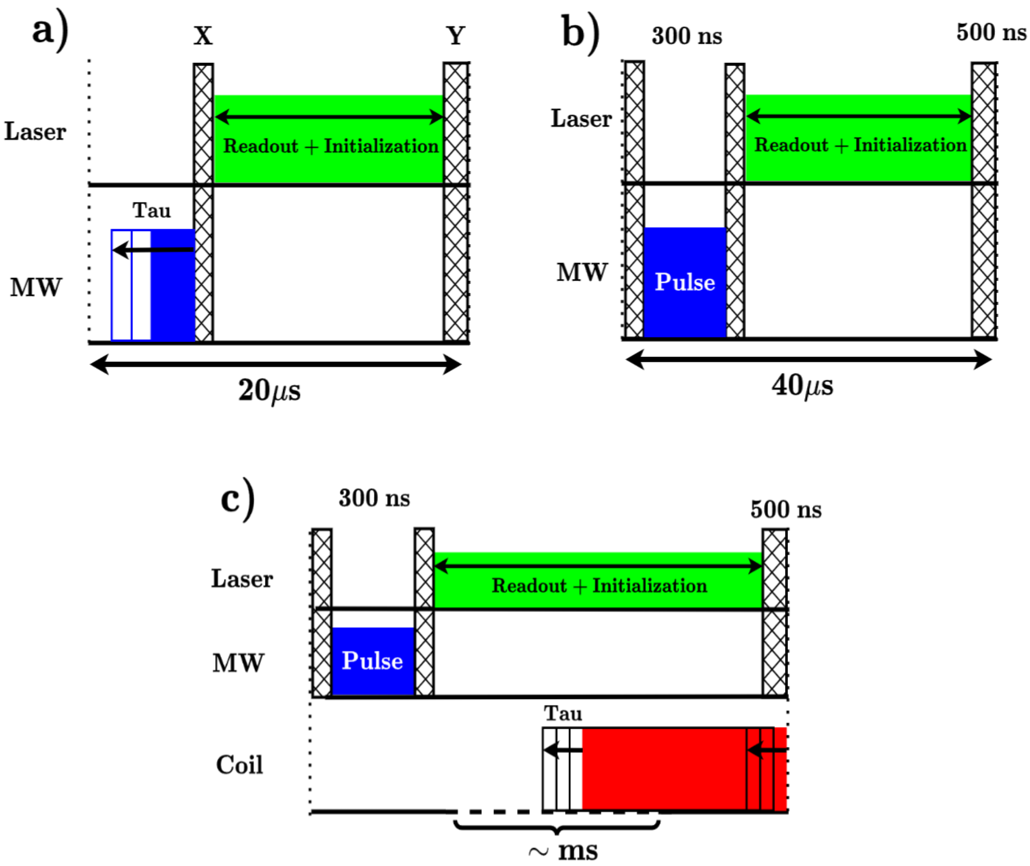

Figure 6: A representation of the pulse schemes for Rabi (a), Pulsed ODMR (b), and Eddy currents (c). The Rabi scheme has variables X and Y, which represent the delay between the microwave and laser, respectively, and the wait between the end of the laser pulse and the next measurement iteration.

3. Results and Discussion

3.1 Rabi

Rabi oscillations are of great importance when operating under pulse conditions. They describe how the spin-state populations oscillate under the influence of an external electromagnetic field. As it is a highly sensitive measurement, the following variables are important and will be investigated.

3.1.1. Laser power

This variable is important as more laser power usually results in higher fluorescence. However, it also brings power-broadening effects. [18] So, the goal is to find the optimal point with enough emission to see contrast while also limiting power broadening. In **Figure 7**, it is visible that at a laser power of 7.5 and 16 mW, no Rabi oscillations occur. Reaching 35 mW and above does result in oscillations. As they are most visible at 45 mW, this laser power will be used for the remainder of the measurements.

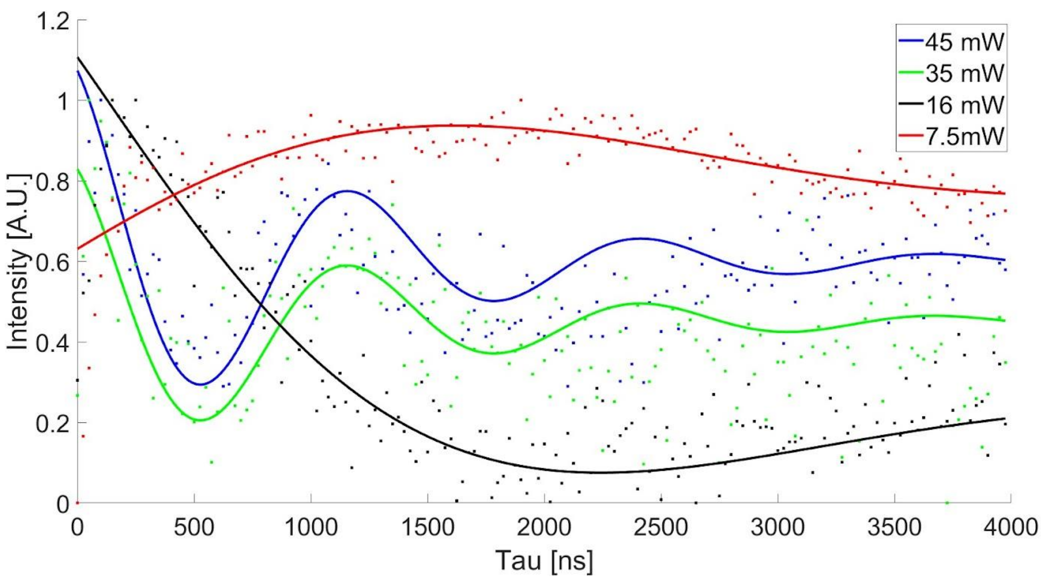

Figure 7: Rabi measurements were performed with different laser powers with a microwave power of 20 dBm. The investigated laser powers are 45 mW (blue), 35 mW (green), 16 mW (black), and 7.5 mW (red).

3.1.2. Microwave frequency used to perform the experiment

As mentioned in the introduction, pulse measurements are more sensitive to the microwave frequency. This means that off-resonant frequencies are less effective in manipulating spin states. To determine the right operating frequency, a CW ODMR spectrum is acquired, and the peaks with the highest contrasts are extracted using a Lorentzian fit. **Figure 8** compares a rabi measurement at on-resonant (2759 MHz) and off-resonant (2730 MHz) frequencies. It is visible that 2759 MHz provides well-defined Rabi oscillations while 2730 MHz shows no sign. Further measurements (until EC) are performed at 2759 MHz.

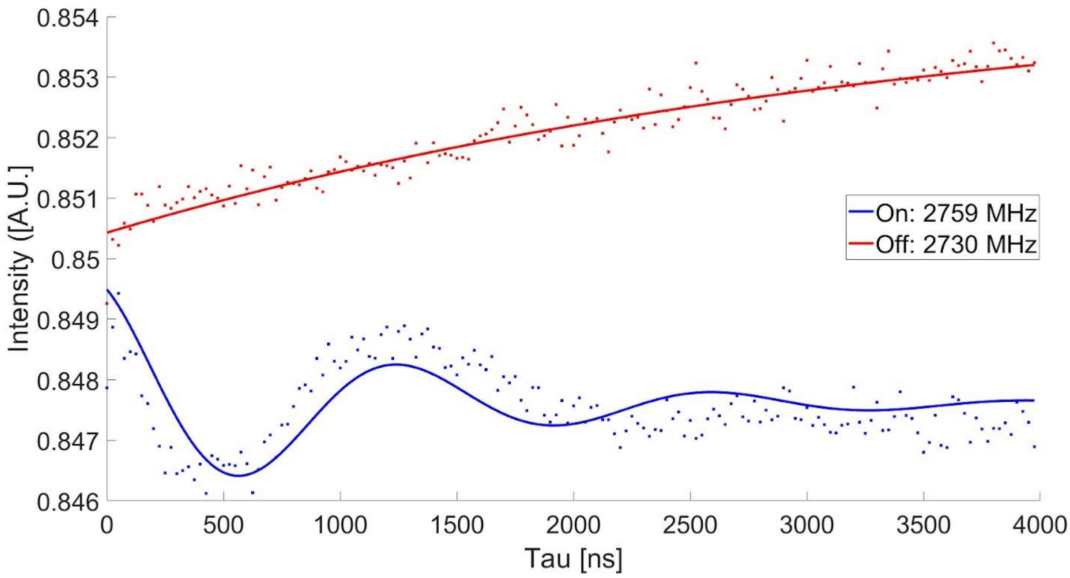

Figure 8: Comparison of on- and off-resonant microwave frequency on Rabi oscillations. Blue is on-resonance and red is off-resonance. The measurement is performed at 20 dBm.

3.1.3. Rabi dependency on microwave power

When performing the Rabi experiment, the power of the applied microwave greatly influences the oscillation times. [19] The aim is to make this effect visible. The investigated powers are 20, 18, 16, and 14 dBm. **Figure 9** shows the power-dependent Rabi measurement. First, it is visible that a decrease in power does result in a lower Rabi frequency. Microwave powers 20 and 18 dBm result in the most pronounced oscillations. This is why future measurements are performed at a microwave power of 20 dBm.

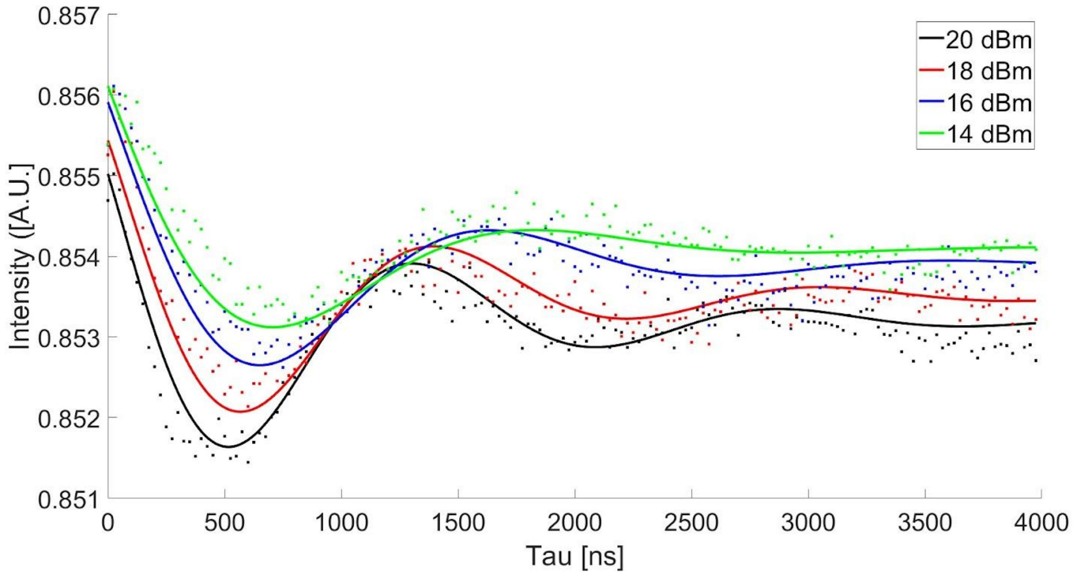

Figure 9: Microwave power-dependent measurements to show that the Rabi oscillation dependency on microwave power. It contains data with powers ranging from 20 dBm to 14 dBm.

3.1.4. Average amount of measurements per datapoint

Working with quantum states requires the user to perform the measurement a multitude of times to get meaningful statistics from the system. With longer experiments, more heating effects can take place. During this study, either 100 or 200 data points were used to calculate an average.

3.1.5. Temperature drift

Lastly, it is preferred that the measurements are taken in an environment that is as stable as possible. When a new measurement is started after an extended time, the first one usually looks like **Figure 10**. This is due to the heating to equilibrium during the first few minutes. While not preferred, temperature fluctuations can be prevented by taking the measurements in quick succession and by discarding the measurements that show this drift.

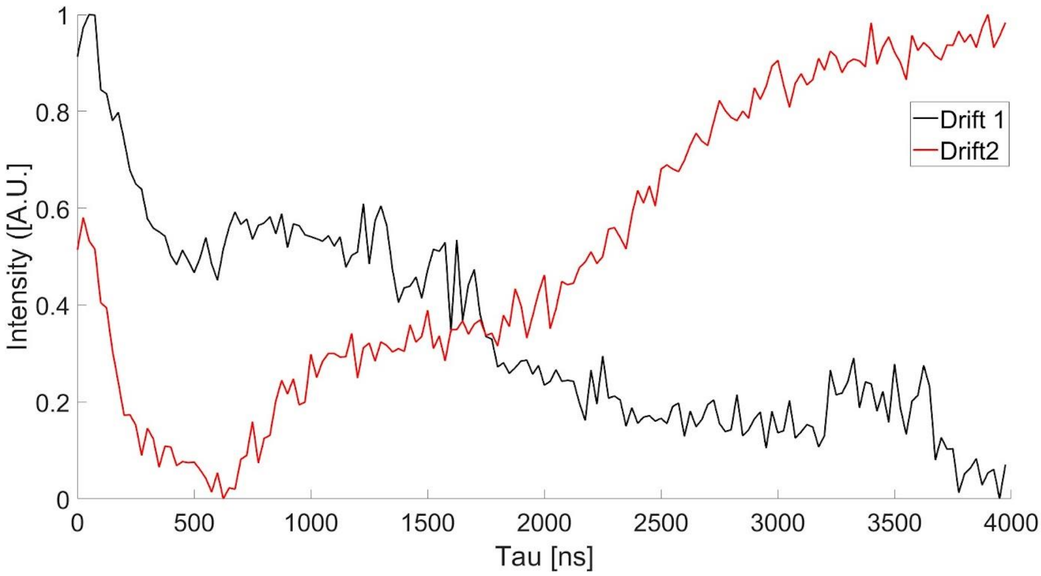

Figure 10: The first measurements performed after an extended period suffers from temperature drifts as the system heats up to equilibrium. The effects of these drifts are shown here, either the intensity increases or decreases. While oscillations are still visible, the non-horizontal drift makes them unusable.

3.2 Pulsed ODMR

Pulsed ODMR measurements are performed on both the initial '405' sample and the one treated with a gold conductive layer. They will be referred to as Sample 1 for the diamond without a gold coating and Sample 2 for the coated one.

Results from Sample 1 are shown in **Figure 11a**. The CW ODMRs are performed at 20 dBm as this is the power used for the pulsed ODMR, 17 dBm to compare it to half the power, and 2.45 dBm calculated from the duty cycle. It is expected that the contrast will remain high while the spectral linewidth decreases. However, as is seen in Figure 11a, this is not the case. There is a significant reduction in contrast without observing the desired linewidth. Similar results are observed when performing pulsed ODMR on sample 2, see Figure 11b. Additionally, the two pulsed measurements are slightly shifted along the frequency axis. A possible cause for this shift is the low microwave power used. At lower power, the noise-to-signal ratio becomes larger, and this could be shown in this way. Next, there are various possibilities for the measurement to become unsuccessful.

First, two sections of the readout pulse are investigated. First is the region where the change in spin population is most visible. This corresponds to the first 200 ns of the readout pulse.

The second region is at the end, where the system should be initialized to the ground state and the emission is constant. When the data is being analyzed, the first section is usually divided by the second to visualize the contrast between them. However, if the laser pulse duration is not long enough, equilibrium will not be reached, and the data can be misinterpreted. So, increasing the laser pulse could express better results. Next, there are some experimental setup changes that can increase sensitivity. These are discussed in section 5 Future outlook.
Despite being unsuccessful, this does not impede this study. The only goal of this measurement is to verify the Rabi variables. However, it does show that further optimization of this pulse scheme is necessary.

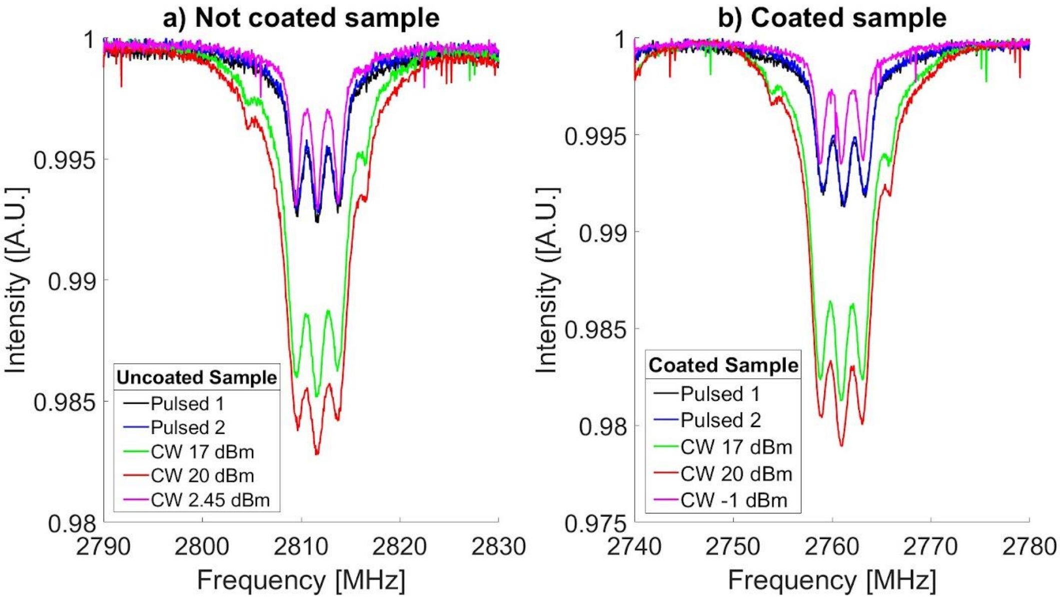

Figure 11: Pulsed ODMR spectrum performed on a) an uncoated diamond and b) a gold-coated diamond. Both are investigated at a microwave pulse power of 20 dBm and compared to continuous ODMR experiments performed at 20 and 17 dBm. Additionally, for both measurement

3.3 Eddy Currents

Figure 12 compares two Eddy current measurements. One where the laser is focused near the conductive layer and a second further away. Due to the different distances, they should be exposed to dissimilar magnitudes of magnetic fields, resulting in a change in decay. This is visible in the data.

When the laser is focused near the conductive layer, the decay occurs faster than at further distances. This can be explained by the Eddy current generation. Being closer results in an increased reduction of the magnetic field over time as the EC works against the field created by the coil. This in turn makes the ODMR resonant peaks return to their original frequency faster. Visible in Figure 12, the red graph.

Similarly, measuring at a higher distance, where the EC field is weaker, will decrease the decay of the resulting field. This figure shows that there is a difference in decay, which proves the concept of this study. Further investigation is needed to optimize the pulse scheme. Changing the coil pulse duration, current, and step size between each measurement are the first steps to be taken toward a better understanding of how to use the diamond magnetometer for material characterization.

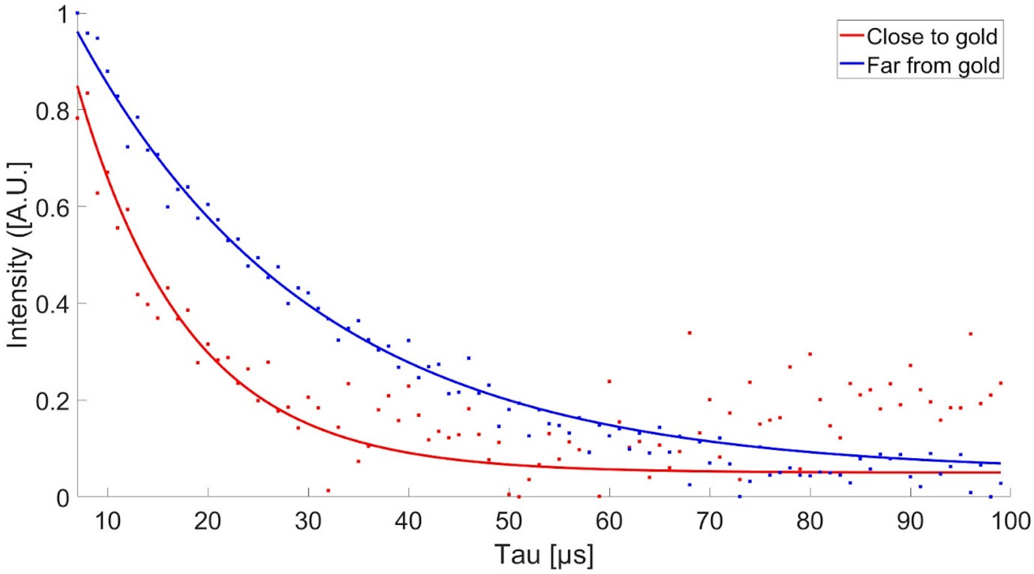

Figure 12: Measurement that analyses the magnetic decay from the coil and conductive sample. By changing the location of the laser spot on the diamond surface, the decay can be investigated either close to the gold layer or further away. The result show a change in decay that can be attributed to the generation of Eddy currents.

4. Conclusion

A new measurement setup was made to measure magnetic fields using a quantum sensor, based on NV centers, in the pulsed regime. Rabi oscillations are detected and parameter optimization has been performed. From these enhanced measurements, the lengths of π-pulse are extracted. For measurements at 20 dBm of microwave power, the π-pulse is 700 ns. With this, pulsed ODMR measurements are performed, but were unsuccessful. Further investigation of the experiment variables and setup improvements are needed. Next, time-resolved Eddy current measurements are performed by applying a current through a coil for two milliseconds and changing its location in time compared to the readout pulses. This measurement showed signs of the detection of EC, proving the concept. Further investigation is needed to extract the conductivity and permeability of materials. Improving the laser path and measuring speed can result in more reliable data and increase sensitivity.

5. Future outlook

Despite proving the concept, a great deal of improvements can be made either to the diamond sample or the measurement setup. The distance from the laser spot to the microwave antenna should be as small as possible. This ensures that the field it creates is most homogeneous. This reasoning can be extended to the magnetic field and the laser. With this, the orientation of the antenna compared to the diamond surface also plays a role. This was found while changing sample 1 with sample 2. On the former, the antenna is placed from one side to the other, while on the latter, the antenna reaches diagonally from corner to corner. Improving the permanent magnetic field will cause the ODMR spectrum to become unique. Next, by reducing the laser spot size, the field is more uniform across the illuminated NV centers, as well as the heat distribution. A known problem with the laser is its elliptical beam shape. Adding optical elements to make it circular will lead to more optimal measuring conditions. In addition to this, altering laser polarity may cause certain NV center orientations to be better addressed, resulting in more contrast. With these adjustments, the laser and microwave powers can be increased to produce more sensitive measurements. The diamond itself can also be improved, as mentioned above. Since sensitivity is affected by T2 decoherence times, increasing this is advantageous. To do so, either reduce the amount of impurities or decouple the NV center from these other defects. Furthermore, increasing the amount of NV centers can also increase sensitivity. However, it is limited by interactions that occur at high NV densities. As a last example of equipment-related improvements, increasing the measurement speed of the detector enables the user to better find the Rabi oscillations.

Everything so far is related to equipment, but the measurement boundaries can also be further investigated. Since the pulsed ODMR was not successful, the boundary conditions should be explored. These contain the duration of the laser pulse, the time between microwave π-pulse and laser pulse, the duration of the MW pulse, etc.

As for the EC, this work was an initial concept study. Changes in the coil design can be investigated as well as the amount of current used when pulsing. Next, both the formation and decay of EC can be studied to determine the characteristics of the conductive sample.

Acknowledgments

First of all, I would like to thank Dr. Jaroslav Hruby for his mentorship during this thesis. His insight and way of explaining really clicked with me, making this an extremely learnful experience. Next, a big thank you to Prof. Dr. Milos Nesladek and Prof. Dr. Anna Ermakova for answering my questions in great detail and providing special equipment. Then, a special thanks to Yarne Beerden and all the OSCAR members for all the good times in the lab, collaborations in certain measurements, and in general the influx of interdisciplinary ideas. Last but not least, I want to thank Aylin Melan. Your support during this thesis and in general this master's has helped me to push through and finalize this amazing study.

References

[1] I. D. Adewale and G. Y. Tian, Decoupling the Influence of Permeability and Conductivity in Pulsed Eddy-Current Measurements, IEEE Trans. Magn. 49, 1119 (2013).

[2] G. Y. Tian, Y. Li, and C. Mandache, Study of Lift-Off Invariance for Pulsed Eddy-Current Signals, IEEE Trans. Magn. 45, 184 (2009).

[3] Nondestructive Inspection Methods, Basic Theory, (2016).

[4] Methods of Controlling Lift-Off in Conductivity Invariance Phenomenon for Eddy Current Testing | IEEE Journals & Magazine | IEEE Xplore, https://ieeexplore.ieee.org/document/9133397.

[5] C. Xu, J. Zhang, H. Yuan, G. Bian, P. Fan, and M. Li, Burst Eddy Current Testing with a Diamond Magnetometry, Appl. Phys. Lett. 120, 084104 (2022).

[6] X. Zhang, G. Chatzidrosos, Y. Hu, H. Zheng, A. Wickenbrock, A. Jerschow, and D. Budker, Battery Characterization via Eddy-Current Imaging with Nitrogen-Vacancy Centers in Diamond, arXiv:2102.11014.

[7] CFQS team et al., Eddy Current Analyses for Vacuum Vessel of CFQS Quasi-Axisymmetric Stellarator, Fusion Eng. Des. 161, (2020).

[8] J. Bashyal, Diamond: Structure, Properties, Types, Applications, https://scienceinfo.com/diamond-structure-properties-types/.

[9] M. Zou, J. Bohon, J. Smedley, J. Distel, K. Schmitt, R.-Y. Zhu, L. Zhang, and E. M. Muller, Proton Radiation Effects on Carrier Transport in Diamond Radiation Detectors, AIP Adv. 10, 025004 (2020).

[10] C. Marquis and A. Zanoni, Nitrogen Vacancy Center Defects in Diamond. Sensor Characterization and Magnetic Field Imaging, https://hdl.handle.net/10589/144251.

[11] R. Schirhagl, K. Chang, M. Loretz, and C. L. Degen, Nitrogen-Vacancy Centers in Diamond: Nanoscale Sensors for Physics and Biology, Annu. Rev. Phys. Chem. 65, 83 (2014).

[12] J. F. Barry, J. M. Schloss, E. Bauch, M. J. Turner, C. A. Hart, L. M. Pham, and R. L. Walsworth, Sensitivity Optimization for NV-Diamond Magnetometry, Rev. Mod. Phys. 92, 015004 (2020).

[13] J.-P. Tetienne, L. Rondin, P. Spinicelli, M. Chipaux, T. Debuisschert, J.-F. Roch, and V. Jacques, Magnetic-Field-Dependent Photodynamics of Single NV Defects in Diamond: Application to Qualitative All-Optical Magnetic Imaging, arXiv:1206.1201.

[14] L. Rondin, J.-P. Tetienne, T. Hingant, J.-F. Roch, P. Maletinsky, and V. Jacques, Magnetometry with Nitrogen-Vacancy Defects in Diamond, Rep. Prog. Phys. 77, 056503 (2014).

[15] E. V. Levine, M. J. Turner, P. Kehayias, C. A. Hart, N. Langellier, R. Trubko, D. R. Glenn, R. R. Fu, and R. L. Walsworth, Principles and Techniques of the Quantum Diamond Microscope, arXiv:1910.00061.

[16] G. Chatzidrosos, A. Wickenbrock, L. Bougas, H. Zheng, O. Tretiak, Y. Yang, and D. Budker, Eddy-Current Imaging with Nitrogen-Vacancy Centers in Diamond, Phys. Rev. Appl. 11, 014060 (2019).

[17] J. Hruby, Diamond NV Colour Centre Spin Resonance Magnetometers: From Fundamentals to Advanced Operation Principles, (2022).

[18] N. V. Vitanov, B. W. Shore, L. Yatsenko, K. Böhmer, T. Halfmann, T. Rickes, and K. Bergmann, Power Broadening Revisited: Theory and Experiment, Opt. Commun. 199, 117 (2001).

[19] H. Shi, J. Ma, X. Li, J. Liu, C. Li, and S. Zhang, A Quantum-Based Microwave Magnetic Field Sensor, Sensors 18, 3288 (2018).